# Metabolic Segregation and Characteristic Gene Clusters of the Key Functional Populations in Anaerobic Digestion Consortia

Yubo Wang[1,2#], Ruoqun Zhang[1], Chunxiao Wang[2], Weifu Yan[2], Tong Zhang[2], Feng Ju[1#]

Author Affiliation:

1. Institute of Advanced Technology, Westlake Institute for Advanced Study, Hangzhou 310024, Zhejiang Province, China

2.Environmental Microbiome Engineering and Biotechnology Laboratory, The University of Hong Kong, Pokfulam, China

[#]Corresponding authors:

Yubo Wang, Email: Y.Wang-43@tudelft.nl, phone: +31(06)17877127

Feng Ju, Email: jufeng@westlake.edu.cn, Ph: +86-571-87380995

**Abstract**

Enrichment experiment integrated with genome-centric meta-omics analysis revealed function partition among populations in the three functional niches of the methanogenic bioprocess: primary fermentation, secondary fermentation (syntrophic acetogenesis) hydrogenotrophic and acetoclastic methanogenesis. Accumulation of $H_2$ as a metabolic intermediate originates mainly from primary fermentation. Formate, rather than $H_2$, plays a key role in secondary fermentation, mediating interspecies electron transfer from the syntrophic oxidizing bacteria to the formate-utilizing methanogens. Such segregation of the electron carrier pools by $H_2$ and formate in primary fermentation and in secondary fermentation, respectively, can benefit the syntrophic oxidizers with a higher tolerance to the accumulation of $H_2$ from the co-occurring primary fermentation. It is interesting to note that, under $H_2$ concentration as high as 50,975 ppm, degradation of either butyrate or propionate was not completely inhibited. Metabolic specificity and characteristic genes/gene clusters are noted for anaerobes of different function niches enriched in this study, i.e., primary fermenting bacteria Clostridium FI21,22, syntrophic butyrate oxidizer in *Syntrophomoas* FI3,4,7, syntrophic propionate oxidizer *Smithellaceae* DES18-25, and formate- and $H_2$-utilizing methanogen *Methanobacteriaceae* EA7.

**Keywords:** Anaerobic digestion, Enriched microbiota, Genome-centric meta-omics, Function partition, Characteristic gene clusters.

## 1. Introduction

Anaerobic digestion (AD) is of central importance in the field of environmental biotechnology since 1980s. It is one of the most cost-effective approaches to stabilize organic components in high-strength waste streams, aiding in bioenergy production and biosolids reduction[1, 2, 3]. However, challenges persist in addressing process upsets such as over-acidification and foam formation[4]. Fine-tuned control and optimization of the AD process depend on a deeper understanding of the sequential microbial reactions mediated by anaerobe populations across the four major functional niches: hydrolysis (conversion of polymers to monomers), primary fermentation/acidogenesis (conversion of monomers to $H_2$/HCOOH, acetate and other reduced fatty acids), secondary fermentation (conversion of reduced fatty acids to acetate and $H_2$/HCOOH) and methanogenesis ($CH_4$ generation mainly from acetate and $H_2$/HCOOH)[5].

Due to the limited amount of energy generated, secondary fermentation is often regarded as the bottleneck step in the AD bioprocess[6]. One of the objectives of this study is to chart the physiology of anaerobes in this specific function niche, specifically, syntrophic butyrate oxidizing bacteria (SBOBs) and syntrophic propionate oxidizing bacteria (SPOBs) in the AD consortia. As key intermediates in the anaerobic mineralization of organic compounds, propionate and butyrate can account for 20-43% of the total methane formation[2].

One of the well-accepted metabolic traits of the SBOBs and the SPOBs is their thermodynamic sensitivity to $H_2$, with an estimated $H_2$ concentration of ~300 ppm being high enough to inhibit the anaerobic oxidation of propionate or butyrate[7]. In the established scheme of methanogenic carbon cycling, the metabolism of almost all substrates, such as carbohydrates and amino acids, generates $H_2$[8]. To our knowledge, there has been little systematic characterization on the dynamics (generation and turnover) of $H_2$ during the AD bioprocess[9] and little evaluation has been conducted on its impact on the conversion of volatile fatty acids (VFAs) beyond theoretical calculations [10]. Inhibition concentration of $H_2$ characterized at 2.03

60 kPa for anaerobic butyrate oxidation and at 11.1 kPa for propionate oxidation are much higher
61 than 300 ppm calculated theoretically [7, 11]. Additionally, evidence is accumulating that suggests
62 that formate plays a more important role than $H_2$ as an interspecies electron carrier in syntrophic
63 oxidation [12]. This study aims to address this knowledge gap by combining the characterization
64 of $H_2$ dynamics with the degradation dynamics of VFAs in lab-scale AD reactors.

65 Full-scale anaerobic digesters rarely harbor high numbers of syntrophic bacteria[3],
66 although they do contain highly abundant primary fermenting populations. Given that
67 syntrophic oxidation of reduced fatty acids proceeds at the thermodynamic limit of life[11],
68 another scientific question to be addressed in this study is: are the SBOBs and SPOBs obligate
69 syntroph, or they more commonly are opportunists capable of fermentation flexibility [11, 13]?
70 Many uncharacterized and uncultivated bacteria in the AD consortia have yet-to-be-identified
71 relationships with the two trophic groups, i.e., primary fermentation *vs.* secondary fermentation,
72 and an in-depth understanding on the metabolic versatility/specificity of the syntrophic
73 populations could help elucidate the intricate ecology that supports the methanogenic
74 conversion of organic compounds.

75 In this study, to obtain consortia dominated by primary fermenting bacteria, SBOBs and
76 SPOBs, enrichment experiment was conducted in three sets of reactors, using glucose, butyrate
77 and propionate as the substrates, respectively. Metabolic versatility of the enriched anaerobes
78 in the three function guilds was evaluated by their metabolic capacity towards and
79 transcriptome response to the presence of either the fermentative substrates (i.e., glucose,
80 fumarate, crotonate) or the reduced short-chain fatty acids (SCFAs, i.e., propionate, butyrate).
81 Dynamics of the generation and turnover of $H_2$ as an intermediate metabolite, and also the
82 impact of $H_2$ accumulation on the syntrophic oxidation of propionate and butyrate, were
83 monitored throughout the batch experiments.

84 **2. Material and methods**

### *2.1 Enrichment of primary fermenting bacteria, SBOBs and SPOBs*

Three sets of AD consortia were enriched for the degradation of glucose, propionate and butyrate, respectively. Duplicate enrichments utilizing each substrate were processed in 1000-ml serum bottles with working volume of 500 ml. Hereafter, the consortia enriched with glucose as substrate will be referred to as 'Consortia-G', the consortia enriched with butyrate as substrate will be referred to as 'Consortia-B', and the consortia enriched with propionate as substrate will be referred to as 'Consortia-P'.

The inoculum used in this enrichment experiment was surplus sludge sampled from Chengxi wastewater treatment plant (Hangzhou, China). A detailed description on the seed sludge used, the feeding strategy, and methods for the physiochemical characterization of the biogas contents and the volatile fatty acids can be found in the supporting information.

### *2.2 Characterization on the metabolic specificity of the primary fermenting bacteria, SBOBs and SPOBs*

To characterize the metabolic specificity of the primary fermenting bacteria, SBOBs and SPOBs, experiment was designed as summarized in Figure S2, to test the metabolic response of the enriched primary fermenting bacteria, SBOBs and SPOBs to different substrates applied. Take the test conducted on SBOBs enriched in Consortia-B as an example: after 219 days enrichment, the 1000 ml (500 ml *2) sludge from two parallel reactors of Consortia-B, in which SBOBs have been enriched, are combined and equally distributed into eight 200 ml serum bottles (each with a 125 ml working volume). In the subsequent batch tests, the primary substrate was sequentially switched from n-butyrate, to propionate, to glucose, to crotonate, and to the combined co-substrate mix of propionate:n-butyrate:glucose (COD:COD:COD=1:1:1). Degradation profile (Figure S3, S4, S5) of the varying substrates by the enriched SBOBs, and transcriptome response of the enriched SBOBs to the varying substrates applied was charted.

### *2.3 Biomass sampling, Nucleic Acid Extraction, and meta-omics analysis*

To profile the succession of the microbial community during the enrichment process, sludge samples were archived weekly to biweekly for sequencing-based analysis. Genomic DNA from the seed sludge (day-0), and from sludge of the enriched consortia collected on day-85, day-134 and day-219 were subjected to metagenome sequencing. When metatranscriptome analysis is relevant, sludge samples (15 ml) collected at each time point were flash frozen in liquid nitrogen and stored in -80 ºC freezer prior to total RNA extraction. Metatranscriptome sequencing was conducted on 20 of the sludge samples collected in section 2.2 (Table S1, Figure S3, S4, S5). A more detailed documentation on the genome-centric meta-omics analysis, the methodologies for 16S rRNA gene (v4-v5 region) based microbiome profiling and the corresponding principal coordinate analysis (PCoA) are provided in the supporting information.

## *3. Results and discussion*

### *3.1 Effects of glucose, butyrate and propionate as the primary substrate on the succession of the anaerobic consortia enriched*

Slow growth rates of the SBOBs and the SPOBs, and the selecting pressure imposed by SCFAs as the primary substrate was reflected by the significant decrease in the volatile suspended solids (VSS, a surrogate measure of the microbial biomass) in the Consortia-B and Consortia-P enriched. As summarized in Figure S6, at the same organic loading rate in terms of COD/L/d, in contrast to ~43% increment in VSS from 8.0 g/L to 11.7 g/l in Consortia-G, both Consortia-B and Consortia-P were observed with a significant decrease in VSS by ~50% from 8.0 g/l to 4.1~4.4 g/l. Despite of the varying VSS contents, equally promising methanogenic conversion of glucose, butyrate and propionate, respectively, was observed in the three consortia, i.e., Consortium-G, Consortia-B and Consortia-P (Figure S1).

A distinct shift in the composition of the microbiome is noted during the enrichment process. A detailed summary on the taxonomy affiliation of the top 15 genera and their relative

135 abundance over the course of the enrichment can be found in Figure 1. Additionally
136 summarized in Figure 2 is the PCoA analysis on the composition of the three consortia enriched.
137 Over the course of the 219-days enrichment, genera that get characteristically enriched in
138 Consortia-G are: *Clostridium sensu stricto3*, *Propionimicrobium* and an unclassified genus in
139 the family of Propionibacteriaceae (g_un_f_Propionibacteriaceae). The one genus that gets
140 characteristically enriched in Consortia-P is *Smithella*, and the one genus that gets
141 characteristically enriched in Consortia-B is *Syntrophomonas*. Herein, we speculate that
142 *Clostridium sensu stricto3*, *Propionimicrobium* and g_un_f_Propionibacteriaceae are primary
143 fermenting bacteria utilizing glucose; *Smithella* is the putative SPOB oxidizing propionate
144 anaerobically, and *Syntrophomonas* the putative SBOB oxidizing butyrate anaerobically.

145 As is summarized in Figure S7-a, after 219 days enrichment, the top 15 genera accounting
146 for 75~83% of the populations in the three enriched consortia are of only ~4% relative
147 abundance in the seed inoculum. Among these top 15 genera are two archaeal methanogen
148 genera: *Methanosaeta* and *Methanobacterium*, and a much higher relative abundance of these
149 two methanogen genera, especially *Methanobacterium* (Figure S7-b), were annotated in
150 Consortia-B (20%) and Consortia-P (22%) than in Consortia-G (6%).

151 ***3.2 Genome-centric identification of the primary fermenting bacteria, SBOBs and SPOBs***
152 ***enriched***

153 317 bacterial metagenome assembled genomes (MAGs) are recovered from the metagenome
154 datasets. A summary of their taxonomy affiliation, their relative abundance and their
155 transcription activity can be found in Figure 3 and Appendix file 1. In the following genome-
156 centric meta-omics analysis, we specifically focus on those 17 bacterial MAGs that have
157 transcription response (>=0.5% of total mRNA clean reads mapped) to at least one of the
158 substrates provided, i.e., glucose, propionate, butyrate, fumarate and crotonate. These 17
159 MAGs include FI21 and FI22 (hereafter, these two MAGs will be referred to as FI21, 22)

160 affiliated with the genus of *Clostridium_T*; DES18, DES19, DES20, DES21, DES22, DES23,
161 DES24, and DES25 (hereafter, these eight MAGs in the same genus of g_Fen_1166 will be
162 referred to as DES18-25) affiliated with the family of *Smithellaceae*; FI3, FI4 and FI7 (hereafter,
163 these three MAGs will be referred to as FI3,4,7) affiliated with the genus of *Syntrophomoas_B*;
164 ER1, ER2 and ER4 (hereafter, these three MAGs will be referred to as ER1,2,4) that are
165 annotatable only at the phylum level as *Eremiobacterota*; and TM1 affiliated with the species
166 *Mesotoga*.

167 Considering that FI21,22 are among the populations that get specifically enriched with
168 glucose as substrate in Consortia-G (datapoint G_DNA in Figure 3), DES18-25 with propionate
169 as substrate in Consortia-P (datapoint P_DNA in Figure 3) and FI3,4 with butyrate as substrate
170 in Consortia-B (datapoint B_DNA in Figure 3), we tentatively assume that FI21, 22 are the
171 primary fermenting bacteria utilizing glucose, FI3,4,7 are the SBOBs degrading butyrate, and
172 DES18-25 are the SPOBs degrading propionate.

173 Function niches of FI21, 22 as the primary fermenting bacteria, FI3,4,7 as SBOBs, and
174 DES18-25 as SPOBs were confirmed by the transcriptome analysis. Specifically, when glucose
175 is provided as the primary substrate to Consortia-G (datapoints gg2 in Figure 3), or as co-
176 substrate to Consortia-B (datapoints bc4 in Figure 3) and Consortia-P (datapoints pc4 in Figure
177 3), FI21, 22 demonstrate the highest transcription activity in all the three consortia enriched,
178 irrespective of their very low abundance in Consortia-B and Consortia-P. Consortia-G cannot
179 use either butyrate or propionate efficiently, probably due to the absence of the SBOB and
180 SPOB populations in the community. When butyrate was provided as the substrate to
181 Consortia-B (datapoint bb4 in Figure 3) or to Consortia-P (datapoint pb5 in Figure 3), FI3,4,7
182 are noted with the highest transcription activity in both consortia. When propionate was
183 provided as the primary substrate to either Consortia-B (datapoint bp5 in Figure 3) or
184 Consortia-P (datapoint pp4 in Figure 3), consistent and relatively high transcription activity of

185 DES18-25 was observed in both consortia.

186 The other four MAGs, ER1,2,4 and TM1, did not show consistent transcriptome response
187 to the presence of any specific substrate tested, and they might be fermentative opportunists in
188 the consortia, utilizing cell debris or other extracellular substances. A more detailed
189 interpretation on the function niches of these four populations can be found in supporting
190 information.

191 ***3.3 Genes and gene clusters mediating either Flavin based electron bifurcation (FBEB) or***
192 ***reverse electron transfer (RET) in primary fermentation, in butyrate oxidation and in***
193 ***propionate oxidation***

194 Transcription patterns of the key functional genes in bacterial MAGs of the three function
195 niches are summarized in Figure 4. And summarized in Table 1 are the genes/gene clusters
196 mediating either the flavin-based electron bifurcation (FBEB) or reverse electron transfer (RET)
197 that are the featuring biochemistry in primary fermentation, syntrophic butyrate oxidation and
198 syntrophic propionate oxidation.

199 The high transcription activity of the FBEB *HydABC* gene cluster in FI21,22 suggests the
200 involvement of electron confurcation of $Fd_{red}$ and NADH for $H_2$ generation during acetate
201 generation (Figure 5a) in primary fermentation of the AD bioprocess where hydrogenotrophic
202 methanogens keep the $H_2$ concentration low.

203 Butyryl-CoA dehydrogenase (*Bcd_EtfAB*) are of high transcription activity in both
204 FI21,22 and in FI3,4,7. In FI21,22, *Bcd_EtfA1B1* neighbors with the GroupB [FeFe]
205 hydrogenase, mediating the NADH-dependent FBEB biochemistry of crotonyl-CoA reduction
206 to butyryl-CoA, and the electrons in the $Fd_{red}$ generated will be further diverted to $H_2$ during
207 butyrate generation in primary fermentation (Figure 5a). In FI3,4,7, *Bcd_EtfA2B2* clusters with
208 the membrane-bound oxidoreductase (*EMO*), mediating the proton motive force (PMF)-
209 dependent RET from butyryl-CoA to membranous methylmenaquinone (MMKH2) [14]. This is

210 one of the featuring biochemistry in anaerobic butyrate oxidation (Figure 5b).

211 The *hydABC* gene cluster is also annotated and with transcription activity in both SBOBs
212 FI3,4,7 and in SPOBs DES18-25 (Figure 4). While comparing with the *hydABC* gene cluster
213 in the primary fermenting bacteria *Clostridium_T* FI21,22, mutations are noted in the *hydB*
214 subunit in the *hydABC* gene cluster of both SBOBs and SPOBs. As visualized in Figure 6, same
215 as that in *S. aciditrophicus* and in *S. wolfei*, the *hydB* subunits in *Syntrophomoas* FI3,4,7 and
216 in *Smithelacea* DES18-25 are all in lack of the C-terminal end 2*[4Fe-4S] function domains.
217 Activity of the FBEB-type *hydABC* requires the presence of both $Fd_{red}$ and NADH [15], while
218 biochemical characterization revealed that enzyme products of the *hydABC* gene cluster in both
219 *S. aciditrophicus* and *S. wolfei* cannot interact with Fdred and can use NADH as direct electron
220 donor for the reduction of $H^+$ [16] [17]. We therefore interpret the *hydABC* gene cluster in
221 *Syntrophomoas* FI3,4,7 and in *Smithelacea* DES18-25 enriched in this study are also of the
222 non-FBEB type and can use NADH as the direct electron donor for $H_2$ generation.

223 The SPOB populations, DES18-25, that get specifically enriched in this study are of a
224 same undefined genus in the family of *Smithelacea.* Propionate conversion via the dismutation
225 pathway, i.e., two propionate molecules being first converted to acetate and butyrate, has been
226 reported only in *Smithella propionica* [18]. And methylmalonyl-CoA pathway is found in all other
227 SPOBs characterized so far [3]. As is summarized in Figure 4, both the presence and transcription
228 activity of genes involved in the β-oxidation of butyrate and in the methylmalonyl-CoA
229 pathway are observed in *Smithelacea* DES18-25.

230 One of the interesting transcription patterns noted in DES18-25 is of the
231 *FdhB_MvhD_HdrABC* gene cluster. Transcription activity and proteome signal of the
232 *FdhB_MvhD_HdrABC* gene cluster in SPOBs have been reported in previous studies [19, 20].
233 There are two hypotheses regarding the function roles of this *FdhB_MvhD_HdrABC* gene
234 cluster and the corresponding enzyme complex: it may either be involved in sulfate reduction

235 [20] or may possess an uncharacterized FBEB activity [19]. We tentatively favor the second
236 hypothesis for two reasons: 1) it was reported that the gram-negative bacteria *Smithella* cannot
237 reduce sulfate [3], further, in this study, to exclude the interference of sulfate as electron acceptor,
238 we replaced $NaSO_4$ with $NaHCO_3$ in the solution medium; and 2) the *FdhB_MvhD_HdrABC*
239 gene cluster showed high transcriptional activity almost exclusively under the presence of
240 propionate as substrate. We cannot exclude the possibility that this *FdhB_MvhD_HdrABC*
241 enzyme complex is relevant in mediating the anaerobic oxidation of succinate to fumarate,
242 which is thermodynamically the most challenging step in anaerobic propionate oxidation *via*
243 the methylmalonyl-CoA pathway [6].

244 Transcription patterns of the key functional genes as summarized in Figure 4 also
245 suggested metabolic specificity of the primary fermenting bacteria, the SBOBs and the SPOBs
246 enriched in this study. A lack of fermentation capacity of the SBOBs and SPOBs was indicated
247 by their quite low transcription activity when fermentative substances (substrate denotated as
248 'S3' in Figure 4) were provided as substrate. In all the three consortia enriched, when glucose
249 was supplied as the primary substrate or as co-substrate, regardless of their either high or low
250 relative abundance in the community, the two fermenting bacteria FI21, 22 were always
251 identified as transcriptionally most active. Specifically, VSS equivalents of FI21,22 were
252 estimated to be of only 13 ug-VSS and 25 ug-VSS in Consortia-B and Consortia-P, respectively
253 (Table S2), being two orders of magnitude lower than that of the putative SBOB populations
254 FI3,4,7 (9817 ug-VSS) in Consortia_B and that of the putative SPOB populations DES18-25
255 (18204 ug-VSS) in Consortia_P; but still, when glucose was provided as co-substrate, this
256 minor amount of FI21,22 dominated in both Consortia_B and Consortia_P the transcription
257 activity of genes involved in glycolysis and pyruvate fermentation (grid M03 in Figure 4), of
258 genes involved in the fatty acid synthesis (grid M04 in Figure 4), and of gene encoding the
259 ferredoxin-dependent [FeFe] hydrogenase during butyrate fermentation (Figure 5a) .

### 3.4 Segregation of $H_2$ and formate metabolism in primary and secondary fermentation

As is discussed in the above section, in primary fermenting bacteria FI21,22, genes encoding hydrogenase ($H_2$ase), i.e., *hydABC* and ferredoxin-dependent [FeFe] $H_2$ase, are annotated and transcribed, mediating electron transfer to $H_2$ during either acetate or butyrate fermentation, and no formate dehydrogenase (*FDH*) was annotated or transcribed. Formate in primary fermentation originates from pyruvate formate lyase (*PFL*), although the transcriptional activity of *PFL* is much lower than that of pyruvate ferredoxin oxidoreductase (*PFOR*), indicating $H_2$ is the dominant electron carrier in primary fermentation.

In contrast, uniquely transcribed in the secondary fermenting populations, i.e., SBOBs FI3,4,7 and SPOBs DES18-22, are *FDH*. The cytosolic formate dehydrogenase (cFDH) catalyze $CO_2/H^+$ reduction to HCOOH with electrons from NADH, while the membrane-bound formate dehydrogenase (mFDH) catalyze proton motive force (PMF)-dependent reverse electron transfer (RET) for $CO_2/H^+$ reduction to HCOOH with electrons from the membranous quinone (M)$MKH_2$. Both cFDH and mFDH are of high transcription activity in SBOBs and SPOBs.

Formate hydrogenlyase (*FHL*) is not annotated or transcribed in either the primary fermenting populations or the secondary fermenting populations. Bacterial *FHL* mediate the conversion of formate to $H_2$, and its absence suggests restricted biochemical interconversion of formate and $H_2$. In other words, metabolism of $H_2$ and formate as electron carriers in anaerobic digestion bioprocess are segregated.

One of the ecological relevance of such segregation of the $H_2$ and formate metabolism in AD bioprocess could be that the '$H_2$-tolerant' primary fermentation and the '$H_2$-sensitive'secondary fermentation can proceed simultaneously, with $H_2$ being the electron carrier in the former, and formate as the predominant electron carrier in the latter. Under high concentrations of $H_2$ emitted from primary fermentation, the '$H_2$-sensitive' secondary fermentation can proceed with formate as dominant electron carrier.

285 Our wet-lab observation aligns well with the genome-centric transcriptome analysis.
286 Accumulation of $H_2$ in high concentrations (5,000-70,000 ppm, Figure S8) was observed only
287 when fermentative substances (i.e., glucose and fumarate) are present as either primary
288 substrate or as co-substrate. $H_2$ accumulation was never detected when only either propionate
289 or butyrate was supplied as the primary substrate.

290 If we assume that $H_2$ is the only electron carrier in the oxidation of propionate and butyrate,
291 at pH=7.0±0.5, (35±1) $^{o}$C, acetate, propionate and butyrate concentration at 10 mM, $CH_4$ and
292 $CO_2$ content in the gaseous phase at 70% and 30% as averaged in this study, the acetogenic
293 oxidation of propionate and butyrate would become thermodynamically unfavorable when the
294 gaseous $H_2$ content is above 132 ppm and 134 ppm, respectively (Figure S9). However, when
295 substrate mix as glucose:propionate:butyrate =1:1:1 (COD:COD:COD) was provided,
296 intermittent $H_2$ accumulation to >30000 ppm was detected in both Consortia-B and Consortia-
297 P, which was far above the theoretical inhibition concentration of $H_2$ as calculated. And at the
298 time points when such high $H_2$ concentrations were detected, the degradation of propionate and
299 butyrate were not completely inhibited, as indicated by the decline of their concentrations
300 summarized in Figure 7.

301 Degradation of propionate and butyrate under high $H_2$ concentrations suggests that $H_2$ is
302 not the sole electron carrier and formate can play a dominant role in mediating interspecies
303 electron transfer during the syntrophic metabolism, which is suggested also by the high
304 transcription activity of *FDH* in SBOBs and SPOBs. However, we did not measure significant
305 accumulation of formate during either butyrate or propionate degradation. Formate
306 concentration below the detection limit (1 mM) is probably due to rapid interspecies formate
307 transfer and efficient utilization of formate by the coupling methanogens in the consortia
308 enriched.

309 ***3.5 Formate- and $H_2$-utilizing methanogen and acetoclastic methanogen identified in the***
310 ***enriched consortia***

311 Among the 39 archaeal MAGs recovered (Figure 7), 4 archaeal MAGs are of the highest
312 transcriptional activity, accounting for (79±9) % of the mRNA gene transcripts mapped to the
313 39 archaeal MAGs. These 4 archaeal MAGs are: EA7 affiliated with the family of
314 *Methanobacteriaceae*, and HA1, HA2, HA3 (hereafter, termed as HA1,2,3) affiliated with the
315 species of *Methanothrix soehngenii*. In the following genome-centric interrogation, we focused
316 specifically on these 4 archaeal MAGs, to elaborate on the methanogenic activity of the
317 enriched consortia.

318 According to the transcription profile as summarized in Figure 8 and Figure S10, EA7 is a
319 formate- and H2- utilizing methanogen and HA1,2,3 are acetoclastic methanogens.
320 *Methanobacteriaceae* EA7 dominated the transcription activity of genes encoding Formate
321 dehydrogenase (coenzyme F420-coupled, denotated as *FdhAB*), formylmethanofuran
322 dehydrogenase (*fwd*), and coenzyme F420 hydrogenase (*frh*). In comparison, *Methanothrix*
323 *soehngenii* HA1,2,3 dominated the mRNA transcripts of genes encoding the acetyl-CoA
324 decarbonylase (*cdhDE*) and the carbon-monoxide dehydrogenase (*cdhAB*). The acetoclastic
325 archaeal MAGs HA1,2,3 are of high identity to strain *Methanothrix soehngenii*, while the
326 hydrogenotrophic archaeal MAG EA7 are annotatable only at the family level of
327 *Methanobacteriacea,* indicating novelty of this hydrogenotrophic methanogen population
328 enriched.

329 Formate as an important electron carrier in the syntrophic cooperation between the
330 SBOB/SPOB and the methanogen archaea is hinted also by the high transcription activity, in
331 EA7, of the *fdhC* gene encoding formate transporter, and also the presence and the high
332 transcription activity of the *FdhAB_mvhD_HdrABC* gene cluster. The formate-centered
333 biochemistry mediated by this *FdhAB_mvhD_hdrABC* enzyme complex is reaction (1). Also

334 annotated in EA7 is the presence and transcription activity of the *MvhAG_MvhD_HdrABC*
335 gene cluster, mediating the $H_2$-centered reaction (2).

336 $$2HCOOH + Fd_{ox} + CoM\text{-}S\text{-}S\text{-}CoB = 2H^+ + 2CO_2 + Fd_{red} + CoM\text{-}SH + CoB\text{-}SH \quad (1)$$

337 $$2H_2 + Fd_{ox} + CoM\text{-}S\text{-}S\text{-}CoB = 2H^+ + Fd_{red} + CoM\text{-}SH + CoB\text{-}SH \quad (2)$$

338 ***3.6 Metabolic specificity of the key functional populations in the AD consortia***

339 According to characterization of the three AD consortia enriched in this study, there is a clear
340 function partition among primary fermentation, syntrophic butyrate oxidation, syntrophic
341 propionate oxidation, hydrogenotrophic methanogenesis, and acetoclastic methanogenesis.
342 Judging by the featuring gene/gene clusters as illustrated in the above sections, function
343 partition among different populations could be clearly seen in Figure 10. In whichever of the
344 three consortia enriched, when butyrate was provided as the primary substrate or as a co-
345 substrate, (100±0) % of the *Bcd_etfAB_EMO* gene transcripts were expressed by the SBOBs.
346 When propionate was provided as the primary substrate or as a co-substrate, (90±5) % of the
347 Succinate dehydrogenase (*Sdh)* gene transcripts were expressed by the SPOBs. When glucose
348 was provided as the primary substrate or as a co-substrate, the primary fermenting populations
349 contributed (97±2)% of the transcripts of genes involved in the glycolysis &fermentation
350 metabolism, e.g., the *PFOR* gene.

351 *cFDH* and *mFDH* were exclusively annotated and transcribed in syntrophic populations
352 (SBOBs FI3,4,7 and SPOBs DES18-22). Coenzyme F420-dependent formate dehydrogenase
353 (*FdhAB*) exclusively in the hydrogenotrophic methanogen EA7. This again highlighted formate
354 as the electron carrier between syntrophic oxidizers and hydrogenotrophic methanogens.

355 The acetoclastic methanogens *Methanothrix* HA1,2,3 and the hydrogenotrophic
356 *Methanobacteriacea* EA7 equally dominant the overall $CH_4$ generation, as these two groups of
357 methanogens each contributed ~50% of the *mcrA* gene transcripts. The *Methanobacteriaceae*
358 EA7 dominated methanogenic conversion of formate and $H_2$ by contributing (95±2) % of the

359 transcripts of the functional genes, e.g., *frhA*, *fdhC* genes. The *Methanothrix soehngenii*
360 HA1,2,3 dominated methanogenic conversion of acetate by contributing (92±4) % of the
361 transcripts of functional genes, e.g., the *cdhA* gene.

362 **Conclusions**

363 Revealed in this study is the segregation of $H_2$- and formate-metabolism in anaerobic digestion
364 bioprocess, with $H_2$ being dominant as electron carrier in primary fermentation, and formate
365 being dominant in secondary fermentation. Such segregation benefit the anaerobic oxidation
366 of butyrate and propionate with higher tolerance to $H_2$ accumulated as metabolic intermediate
367 from primary fermentation.

368 Metabolic specificity was noted for the key functional populations in the AD consortia.
369 Genome-centric transcriptional characterization highlighted the characteristic genes/gene
370 clusters of the different functional groups. specifically, *Bcd_etfAB_H₂ase* in primary
371 fermenting bacteria *Clostridium_T*, *Bcd_etfAB_EMO* in the syntrophic butyrate-oxidizing
372 bacteria (SBOBs) in the genus of *Syntrophomonas_B*, *Sdh* and *FdhB_mvhD_hdrABC* in the
373 syntrophic propionate-oxidizing bacteria (SPOBs) affiliated to *Smithellaceae*,
374 *FdhC_FdhAB_mvhD_hdrABC* and *mvhABG_mvhD_hdrABC* in the one hydrogenotrophic
375 methanogen affiliated to *Methanobacteriaceae*, and *cdhA* in the acetoclastic methanogen
376 species *Methanothrix soehngenii*.

377 Genome-centric interpretation at the level of gene clusters can deliver higher resolution
378 in genotype-phenotype correlation. At the gene cluster level, genetic machineries of primary
379 fermenting bacteria generating butyrate and SBOB degrading butyrate can be distinguished. A
380 membrane-bound EMO subunit neighboring with etfAB subunits is essential for reverse
381 electron transfer in SBOB.

382 Mutations in the *hydB* subunit are noted in the *hydABC* gene cluster of both
383 *Syntrophomonas_B* SBOBs and *Smithellaceae* SPOBs enriched in this study. Such mutations

probably render $H^+$ reduction by NADH as direct electron donor during syntrophic oxidation of butyrate and metabolism. And only the *hydABC* enzyme complex in primary fermenting bacteria are of true FBEB activity and can interact with both NADH and $Fd_{red}$ for $H^+$ reduction.

**Data Availability Statement**

Metagenome DNA (10 datasets in total) and metatranscriptome RNA (20 data sets in total) sequencing data are available in the NCBI Sequence Read Achieve (SRA) database under the Bioproject accession number of PRJNA886957. The 17 bacterial MAGs and 4 archaeal MAGs analyzed in this study are accessible in NCBI under the Bioproject accession number of PRJNA886046, function genes annotated in these 21 MAGs and their transcription activity could be found in Appendix file 1. 16S rRNA gene amplicon sequences (v4-v5 region) have also been deposited in NCBI under the Bioproject accession number of PRJNA885972.

**Declaration of Competing Interest**

The authors declare that there is no competing interest.

**Abbreviations**

SBOBs - syntrophic butyrate oxidizing bacteria; SPOBs - syntrophic propionate oxidizing bacteria; AD - anaerobic digestion; VFAs - volatile fatty acids; SCFAs - short-chain fatty acids; COD - chemical oxygen demand; PCoA - principle coordinate analysis; VSS - volatile suspended solids; MAGs - metagenome assembled genomes; FBEB – flavin based electron bifurcation; RET – reverse electron transfer; PMF – proton motive force; PFL – pyruvate formate lyase; PFOR – pyruvate ferredoxin oxidoreductase; FHL – formate hydrogenlyase; EMO – membrane-bound oxidoreductase.

**Acknowledgments**

This work was supported by the Zhejiang Provincial Natural Science Foundation of China under Grant No. LR22D010001 and Key R&D Program of Zhejiang (2022C03075) and Research Center for Industries of the Future (RCIF). Technical assistance from Ms. Yisong Xu

in laboratory affairs and Mr. Guoqing Zhang in maintaining the in-house computing facility are greatly appreciated.

**Authors' contributions**

YW conceptualized the research and discussed with FJ. YW conducted the wet-lab experiment, the meta-omics data analysis, and wrote the manuscript. RZ assisted with the wet-lab experiment. CW, WY, TZ and FJ contributed in the interpretation of the results and revision of the manuscript.

416 **Table1.** Presence (+) and absence(-) of the gene clusters mediating either flavin based electron bifurcation (FBEB) or reverse electron transfer
417 (RET) in primary fermentation and in syntrophic oxidation of butyrate and propionate, their cellular component and the corresponding
418 biochemistry**.**

| **Gene/ Gene clusters** | **Cellular component** | **Biochemistry** | **Primary fermenting bacteria** | **SBOB** | **SPOB** |
|---|---|---|---|---|---|
| | | | FI21,22 | FI3,4,7 | DES18-25 |
| *hydA_hydB_hydC* | Cytoplasm | $Fd_{red} + NADH + 4H^+ = 2H_2 + NAD^+ + Fd_{ox}$ (in primary fermentation); OR $NADH + 2H^+ = H_2 + NAD^+$ (in syntrophic oxidation) | + | + | + |
| *Bcd_EtfA_EtfB_H₂ase* | Cytoplasm | $2NADH + Crotonyl\text{-}CoA + Fd_{ox} = 2\ NAD^+ + Butyryl\text{-}CoA + Fd_{red}$ | + | - | - |
| *cFDH* | Cytoplasm | $NADH + CO_2 + H^+ = NAD^+ + HCOOH$ | - | + | + |
| *mFDH* | Membrane-bound | $(M)MKH_2 + CO_2 + PMF = HCOOH + (M)MK$ | - | + | + |
| *FdhB_mvhD_HdrABC* | Cytoplasm | UNKNOWN | - | - | + |
| *Bcd_EtfB_EMO_EtfA* | Membrane-bound | $Butyryl\text{-}CoA + MMK + PMF = Crotonyl\text{-}CoA + MMKH_2$ | - | + | - |
| *SdhA_SdhB_SdhC* | Membrane-bound | $Succinate + (M)MK + PMF = Fumarate + (M)MKH_2$ | - | - | + |

419

420 **Figure list**

421 **Figure 1.** Taxonomy affiliation and relative abundance of the top 15 genus in the three consortia
422 enriched with glucose, propionate and butyrate, respectively. Summarized in this figure are the
423 16S rRNA gene (v4-v5 region) based microbiome profile in Consortia-G Consortia-B and
424 Consortia-P from day 37 to day 219, and in seed sludge on day 0.
425 **Figure 2.** Principal coordinates analysis (PCoA) of the three anaerobic digestion consortia
426 enriched with glucose, propionate and butyrate, respectively. The community structures were
427 inferred from the 16S rRNA amplicon sequence variants (v4-v5 region), and the PCoA analysis
428 is based on the euclidean distance matrix. PCoA1 and PCoA2 are shown with the percentage
429 variation explained for each axis. During the course of the 219 days enrichment, the most
430 varying component in Consortia-G were genus *Clostridium sensu stricto* 3, *Propionimicrobium*,
431 and an unclassified genus in the family of *Propionibacteriacea*; the most varying component
432 in Consortia-P was the genus *Smithella*, and the most varying component in Consortia-B was
433 the genus *Syntrophomonas*.
434 **Figure 3.** Maximum likelihood tree of the 315 bacterial MAGs recovered in this study. The
435 inner heatmap summarized the meta-DNA based abundance and the meta-RNA based
436 transcription activity of each MAG. 'seed_DNA', 'B_DNA', 'P_DNA' and 'G_DNA' denoted
437 meta-DNA based abundance of each MAG in the seed sludge, in the enriched Consortia-G,
438 Consortia-B and Consortia-P, respectively; and the other datapoints are of the meta-RNA based
439 transcription activity of each MAG. A detailed information on each meta-RNA datapoint could
440 be found in Table S1 and Figure S3-S5. The 17 MAGs highlighted with white bold labels were
441 those MAGs annotated with relatively high transcription activity in response to certain
442 substrates provided. The tree was constructed using FastTree [21] (maximum-
443 likelihood phylogeny) based on a set of 120 concatenated universal single-copy
444 proteins for Bacteria [22]. Branches of the phylogenetic tree are coloured according to their
445 taxonomy affiliation at the phylum level, and those grey dots at each inner node indicate
446 bootstrap values >=0.9.
447 **Figure 4.** Transcription activity of the key functional genes annotated in the 17 MAGs in
448 response to the stimuli of varying substrates in A) Consortia-B, B) Consortia-P and C)
449 Consortia-G. FI3,4,7 refers to the three putative SBOBs in the genera of *Syntrophomonas_B*,
450 DES18-25 refers to the eight putative SPOBs of the same unnamed genera in the family of
451 Smithellaceae, FI21,22 refers to the two putative fermenting bacteria in the genera of
452 *Clostridium_T*, TM1 refers to the one *Mesotoga* MAG, and ER1,2,4 refers to the 3 co-occurring
453 Eremiobacterota MAGs. S1, S2 and S3 listed horizontally denotated the stimuli of varying
454 substrates, i.e., n-butyrate, propionate and fermentative substrate, respectively. The
455 fermentative substrate is glucose in Consortia-G, fumarate in Consortia-P and crotonate in
456 Consortia-B. Sc denoted the stimuli of combined substrate as glucose: propionate:
457 butyrate=1:1:1 (COD:COD:COD). $ScH_2$ and $S3H_2$ refer to the datapoints when there is
458 accumulation of $H_2$, when glucose was present as either co-substrate or the primary substrate.
459 Colours of the circles indicate change of the transcription activity of the corresponding genes,
460 in log difference relative to that before the stimuli of the corresponding substrate (datapoint g0,
461 b0 and p0 as summarized in Table S1); and the size of the circles indicate the square root of the
462 RNA-RPKM values of the corresponding genes. Clustered in M01 are key genes involved in
463 butyrate oxidation, in M02 are key genes involved in propionate oxidation, in M03 are key
464 genes involved in the glycolysis and pyruvate metabolism, in M04 are key genes involved in
465 the fatty acid synthesis, in M05 are the Fdh-N type and Fdh-H type formate dehydrogenase, in

M06 are hydrogenase genes, in M07 are genes encoding the the electron transfer flavoprotein, in M08 is the ATP synthase gene, in M09 are genes encoding the type IV pili, flagellar and fimbria assembly protein, in M10 are genes encoding the protease, murein-degrading enzymes and amylase etc., in M11 are genes encoding the synthesis of protein, amino acids, and glycogen. Full names of genes denoted with abbreviations could be found in the Appendix file 1.

**Figure 5.** a) Acetate and butyrate metabolism in primary fermenting bacteria *Clostridium* FI21,22 and the corresponding gene clusters encoding enzymes mediating the flavin-based electron bifurcation; b) proton motive force (PMF) dependent butyryl-CoA oxidation to crotonyl-CoA, the biochemistry and the corresponding gene clusters.

**Figure 6.** Summary of the function domains in the *hydB* subunit in the flavin based electron bifrucation (FBEB) type of *hydABC* in the primary fermenting populations (upper box) and in the non-FBEB type *hydABC* in the secondary fermenting populations. Name of the reference microbe strains in which the catalytic activity of the enzyme complex has been characterized are highlighted in blue. Names of the anaerobe populations enriched in study are shown in grey. Provided in the brackets are the gene accession number of the corresponding *hydB* gene.

**Figure 7.** Degradation profile of propionate (HPr) and butyrate (HBut), and dynamics of $H_2$ concentration when glucose:propionate:butyrate = 1:1:1 (COD:COD:COD) was provided as substrate in a) Consortia-P, b) Consortia-B, and c) Consortia-G. d) Gibbs free energy change calculated for the degradation of propionate, n-butyrate and iso-butyrate in Consortia-P and Consortia-B , respectively, assuming that $H_2$ is the only electron carrier generated from the syntrophic oxidation of butyrate or propionate.

**Figure 8.** Maximum likelihood tree of the 39 archaeal MAGs recovered in this study. The inner heatmap summarized the meta-RNA based transcription activity of each MAG. A detailed information on each meta-RNA datapoint could be found in Table S1. The tree was constructed using FastTree (maximum-likelihood phylogeny) [21] based on a set of 122 concatenated universal single-copy proteins for *Archaea* [22]. Branches of the phylogenetic tree are coloured according to their taxonomy affiliation, and those light purple dots indicate bootstrap values >=0.9.

**Figure 9.** Transcription activity of the key functional genes annotated in the Methanobacteriaceae MAG EA7, and in the three *Methanothrix* MAGs HA1,2,3. The heatmap represents the transcription activity of the corresponding genes, and the data given alongside the heatmap bar are square root of the RNA-RPKM values. Full names of genes denoted with abbreviations could be found in the Appendix file 1. Genes grouped in grid R1 are those specifically involved in hydrogenotrophic methanogenesis, genes grouped in grid R2.1-R2.3 are those specifically involved in acetoclastic methanogenesis, and genes grouped in grid R3 are genes shared by both the hydrogenotrophic methanogenesis and acetoclastic methanogenesis

**Figure 10.** Contribution of the putative fermenter bacteria (*Clostridium_T* FI21,22), the putative SBOBs (*Syntrophomonadaceae* FI3,4,7), the putative SPOBs (*Smithellaceae*, DES18-25) to the mRNA transcripts of the core genes (left, coloured by genes) involved in the butyrate metabolism (*EtfAB_EMO*), the propionate metabolism (*Sdh*, Succinate dehydrogenase) and the pyruvate fermentation (*PFOR,* Pyruvate-ferredoxin oxidoreductase), under the stimuli of butyrate, propionate and glucose, respectively. And also, when there is no $H_2$ accumulation, contribution of *Methanobacteriaceae* EA7 and *Methanothrix_soehngenii* HA1,2,3 to the mRNA transcripts of the core genes involved in the methanogenesis metabolism, i.e., *fdhA*: formate dehydrogenase (coenzyme F420) alpha subunit, *fdhC*: formate transporter, *cdhA*: acetyl-CoA decarbonylase, and *mcrA*: methyl coenzyme M reductase. Colours represent different genes, and the width of each ribbon represents the contribution ratios of each microbe group to the mRNA transcripts of each gene, the ratios were averaged across the stimuli results

516 in the three enriched consortia: Consortia-G, Consortia-B and Consortia-P. cFDH and mFDH
517 refer to the cytosolic and membrane-bound formate dehydrogenase, respectively.

## References

(1) Ariesyady, H. D.; Ito, T.; Okabe, S. Functional bacterial and archaeal community structures of major trophic groups in a full-scale anaerobic sludge digester. *Water Res* **2007**, *41* (7), 1554-1568. DOI: 10.1016/j.watres.2006.12.036. Jain, M. Anaerobic Membrane Bioreactor as Highly Efficient and Reliable Technology for Wastewater Treatment—A Review. *Advances in Chemical Engineering and Science* **2018**, *08* (02), 82-100. DOI: 10.4236/aces.2018.82006. Speece, R. E. Anaerobic biotechnology for industrial wastewater treatment. *ES&T Features* **1983**, *17* (9), 416-417. DOI: 10.1021/es00115a001,. Macarie, H. Overview of the application of anaerobic treatment to chemical and petrochemical wastewaters. *Water Science and Technology* **2000**, *42* (5-6), 201-214. DOI: 10.2166/wst.2000.0515.

(2) Bryant, R. I. M. a. M. P. Metabolic activity of fatty acid-oxidizing bacteria and the contribution of acetate, propionate, butyrate and CO2 to methanogenesis in cattle waste at 40 and 60 ºC. *Applied and Environmental Microbiology* **1981**, *41* (6), 1363-1373.

(3) Stams, A. J.; Sousa, D. Z.; Kleerebezem, R.; Plugge, C. M. Role of syntrophic microbial communities in high-rate methanogenic bioreactors. *Water Sci Technol* **2012**, *66* (2), 352-362. DOI: 10.2166/wst.2012.192 From NLM Medline.

(4) Moeller, L.; Zehnsdorf, A. Process upsets in a full-scale anaerobic digestion bioreactor: over-acidification and foam formation during biogas production. *Energy, Sustainability and Society* **2016**, *6* (1). DOI: 10.1186/s13705-016-0095-7.

(5) C.Adinarayana Reddy, M. P. B., M.J.Wolin. Characteristics of S Organism Isolated from Methanobacillus omelianskii. *Journal of Bacteriology* **1972**, *109* (2), 539-545. McInerney, M. J.; Struchtemeyer, C. G.; Sieber, J.; Mouttaki, H.; Stams, A. J.; Schink, B.; Rohlin, L.; Gunsalus, R. P. Physiology, ecology, phylogeny, and genomics of microorganisms capable of syntrophic metabolism. *Ann N Y Acad Sci* **2008**, *1125*, 58-72. DOI: 10.1196/annals.1419.005 From NLM Medline. Michael J. McInerney, M. P. B., and Norbert Pfenning. Anaerobic Bacterium that Degrades Fatty Acids in Syntrophic Association with Methanogens. *Archives of Microbiology* **1979**, *122*, 129-135. Narihiro, T.; Nobu, M. K.; Kim, N. K.; Kamagata, Y.; Liu, W. T. The nexus of syntrophy-associated microbiota in anaerobic digestion revealed by long-term enrichment and community survey. *Environ Microbiol* **2015**, *17* (5), 1707-1720. DOI: 10.1111/1462-2920.12616. Nobu, M. K.; Narihiro, T.; Rinke, C.; Kamagata, Y.; Tringe, S. G.; Woyke, T.; Liu, W. T. Microbial dark matter ecogenomics reveals complex synergistic networks in a methanogenic bioreactor. *ISME J* **2015**, *9* (8), 1710-1722. DOI: 10.1038/ismej.2014.256. Rudolf K. Thauer, K. J., Karl Decker. Energy Conservation in Chemotrophic Anaerobic Bacteria. *Bacteriological Reviews* **1977**, *41* (1), 100-180. Schink, B. Energetics of Syntrophic Cooperation in Methanogenic Degradation.

*Microbiology and Molecular Biology Reviews* **1997**, *61* (2), 262-280.
(6) Westerholm, M.; Calusinska, M.; Dolfing, J. Syntrophic propionate-oxidizing bacteria in methanogenic systems. *FEMS Microbiol Rev* **2022**, *46* (2). DOI: 10.1093/femsre/fuab057 From NLM Medline.
(7) Nobu, M. K.; Narihiro, T.; Mei, R.; Kamagata, Y.; Lee, P. K. H.; Lee, P. H.; McInerney, M. J.; Liu, W. T. Catabolism and interactions of uncultured organisms shaped by eco-thermodynamics in methanogenic bioprocesses. *Microbiome* **2020**, *8* (1), 111. DOI: 10.1186/s40168-020-00885-y.
(8) de Kok, S.; Meijer, J.; van Loosdrecht, M. C.; Kleerebezem, R. Impact of dissolved hydrogen partial pressure on mixed culture fermentations. *Appl Microbiol Biotechnol* **2013**, *97* (6), 2617-2625. DOI: 10.1007/s00253-012-4400-x From NLM Medline.
(9) Birgitte K. Ahring, P. W. Kinetics of Butyrate, Acetate, and Hydrogen Metabolism in a Thermophilic, Anaerobic, Butyrate-Degrading Triculture. *Appl Environ Microbiol* **1987**, *53*, 434-439.
(10) R. Conrad, B. S., and T.J. Phelps. Thermodynamics of $H_2$-consuming and H2-producing metabolic reactions in diverse methanogenic environments under in situ conditions. *FEMS Microbiol Eco* **1986**, *38*, 353-360.
(11) Sieber, J. R.; McInerney, M. J.; Gunsalus, R. P. Genomic insights into syntrophy: the paradigm for anaerobic metabolic cooperation. *Annu Rev Microbiol* **2012**, *66*, 429-452. DOI: 10.1146/annurev-micro-090110-102844 From NLM Medline.
(12) de Bok, F. A.; Luijten, M. L.; Stams, A. J. Biochemical evidence for formate transfer in syntrophic propionate-oxidizing cocultures of Syntrophobacter fumaroxidans and Methanospirillum hungatei. *Appl Environ Microbiol* **2002**, *68* (9), 4247-4252. DOI: 10.1128/AEM.68.9.4247-4252.2002 From NLM Medline. Leslie A. Day, E. L. K., Dallas R. Fonseca, Kyle C. Costa. Interspecies Formate Exchange Drives Syntrophic Growth of Syntrophotalea carbinolica and Methanococcus maripaludis. *Appl Environ Microbiol* **2022**, *88*.
(13) Worm, P.; Koehorst, J. J.; Visser, M.; Sedano-Nunez, V. T.; Schaap, P. J.; Plugge, C. M.; Sousa, D. Z.; Stams, A. J. M. A genomic view on syntrophic versus non-syntrophic lifestyle in anaerobic fatty acid degrading communities. *Biochim Biophys Acta* **2014**, *1837* (12), 2004-2016. DOI: 10.1016/j.bbabio.2014.06.005 From NLM Medline.
(14) Agne, M.; Estelmann, S.; Seelmann, C. S.; Kung, J.; Wilkens, D.; Koch, H. G.; van der Does, C.; Albers, S. V.; von Ballmoos, C.; Simon, J.; et al. The missing enzymatic link in syntrophic methane formation from fatty acids. *Proc Natl Acad Sci U S A* **2021**, *118* (40). DOI: 10.1073/pnas.2111682118 From NLM Medline.
(15) Buckel, W.; Thauer, R. K. Flavin-Based Electron Bifurcation, A New Mechanism of Biological Energy Coupling. *Chem Rev* **2018**, *118* (7), 3862-3886. DOI:

10.1021/acs.chemrev.7b00707 From NLM Medline.
(16) Losey, N. A.; Mus, F.; Peters, J. W.; Le, H. M.; McInerney, M. J. Syntrophomonas wolfei Uses an NADH-Dependent, Ferredoxin-Independent [FeFe]-Hydrogenase To Reoxidize NADH. *Appl Environ Microbiol* **2017**, *83* (20). DOI: 10.1128/AEM.01335-17 From NLM Medline.
(17) Losey, N. A.; Poudel, S.; Boyd, E. S.; McInerney, M. J. The Beta Subunit of Non-bifurcating NADH-Dependent [FeFe]-Hydrogenases Differs From Those of Multimeric Electron-Bifurcating [FeFe]-Hydrogenases. *Front Microbiol* **2020**, *11*, 1109. DOI: 10.3389/fmicb.2020.01109 From NLM PubMed-not-MEDLINE.
(18) Yitai Liu, D. L. B., Henry C. Aldrich, Gwendolyn R. Drake, David R. Boone. Characterization of the anaerobic propionate-degrading syntrophs Smithella propionica gen. nov., sp. nov. and Syntrophobacter wolinii. *International Journal of Systematic Bacteriology* **1999**, *49*, 545-556. de Bok, F. A.; Stams, A. J.; Dijkema, C.; Boone, D. R. Pathway of propionate oxidation by a syntrophic culture of Smithella propionica and Methanospirillum hungatei. *Appl Environ Microbiol* **2001**, *67* (4), 1800-1804. DOI: 10.1128/AEM.67.4.1800-1804.2001 From NLM Medline.
(19) Sedano-Nunez, V. T.; Boeren, S.; Stams, A. J. M.; Plugge, C. M. Comparative proteome analysis of propionate degradation by Syntrophobacter fumaroxidans in pure culture and in coculture with methanogens. *Environ Microbiol* **2018**, *20* (5), 1842-1856. DOI: 10.1111/1462-2920.14119 From NLM Medline.
(20) Hao, L.; Michaelsen, T. Y.; Singleton, C. M.; Dottorini, G.; Kirkegaard, R. H.; Albertsen, M.; Nielsen, P. H.; Dueholm, M. S. Novel syntrophic bacteria in full-scale anaerobic digesters revealed by genome-centric metatranscriptomics. *ISME J* **2020**, *14* (4), 906-918. DOI: 10.1038/s41396-019-0571-0 From NLM Medline.
(21) Price, M. N.; Dehal, P. S.; Arkin, A. P. FastTree: computing large minimum evolution trees with profiles instead of a distance matrix. *Mol Biol Evol* **2009**, *26* (7), 1641-1650. DOI: 10.1093/molbev/msp077.
(22) Chaumeil, P. A.; Mussig, A. J.; Hugenholtz, P.; Parks, D. H. GTDB-Tk: a toolkit to classify genomes with the Genome Taxonomy Database. *Bioinformatics* **2019**. DOI: 10.1093/bioinformatics/btz848.

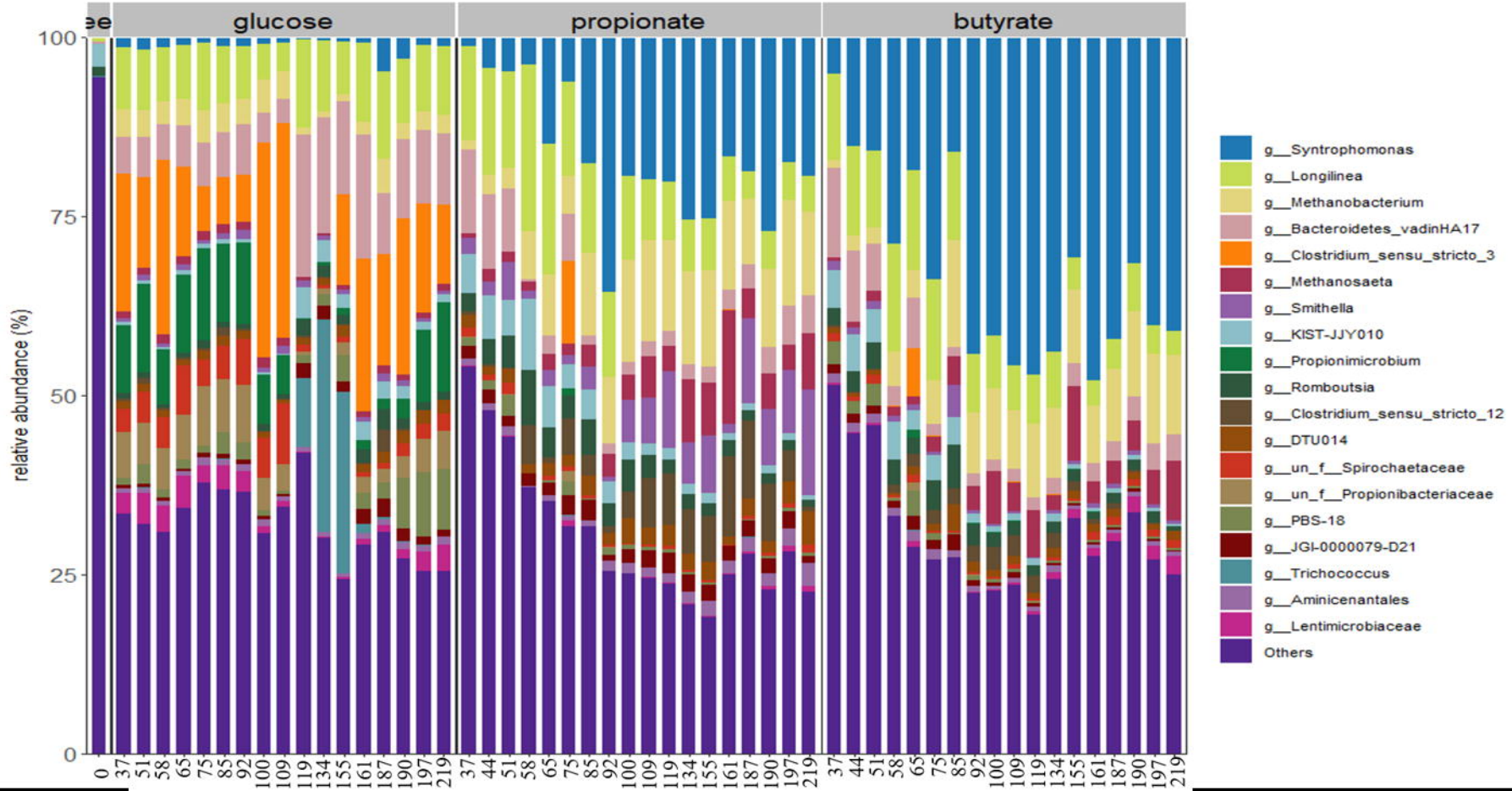
glucose
propionate
butyrate
relative abundance (%)
100
75
50
25
0
g__Syntrophomonas
g__Longilinea
g__Methanobacterium
g__Bacteroidetes_vadinHA17
g__Clostridium_sensu_stricto_3
g__Methanosaeta
g__Smithella
g__KIST-JJY010
g__Propionimicrobium
g__Romboutsia
g__Clostridium_sensu_stricto_12
g__DTU014
g__un_f__Spirochaetaceae
g__un_f__Propionibacteriaceae
g__PBS-18
g__JGI-0000079-D21
g__Trichococcus
g__Aminicenantales
g__Lentimicrobiaceae
Others

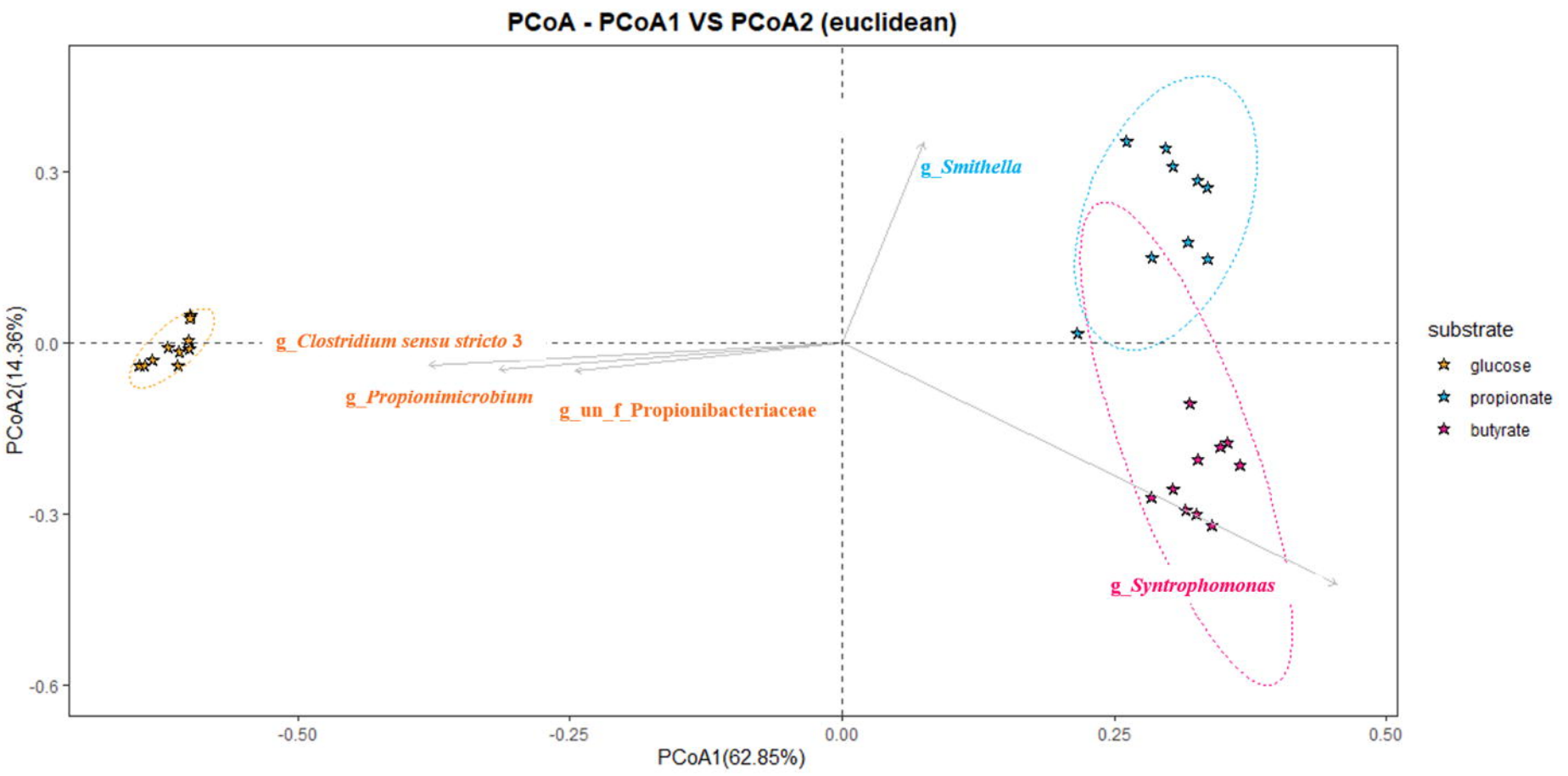
PCoA - PCoA1 VS PCoA2 (euclidean)
g_Smithella
g_Clostridium sensu stricto 3
g_Propionimicrobium
g_un_f_Propionibacteriaceae
g_Syntrophomonas
substrate
glucose
propionate
butyrate
PCoA2(14.36%)
PCoA1(62.85%)
0.3
0.0
-0.3
-0.6
-0.50
-0.25
0.00
0.25
0.50

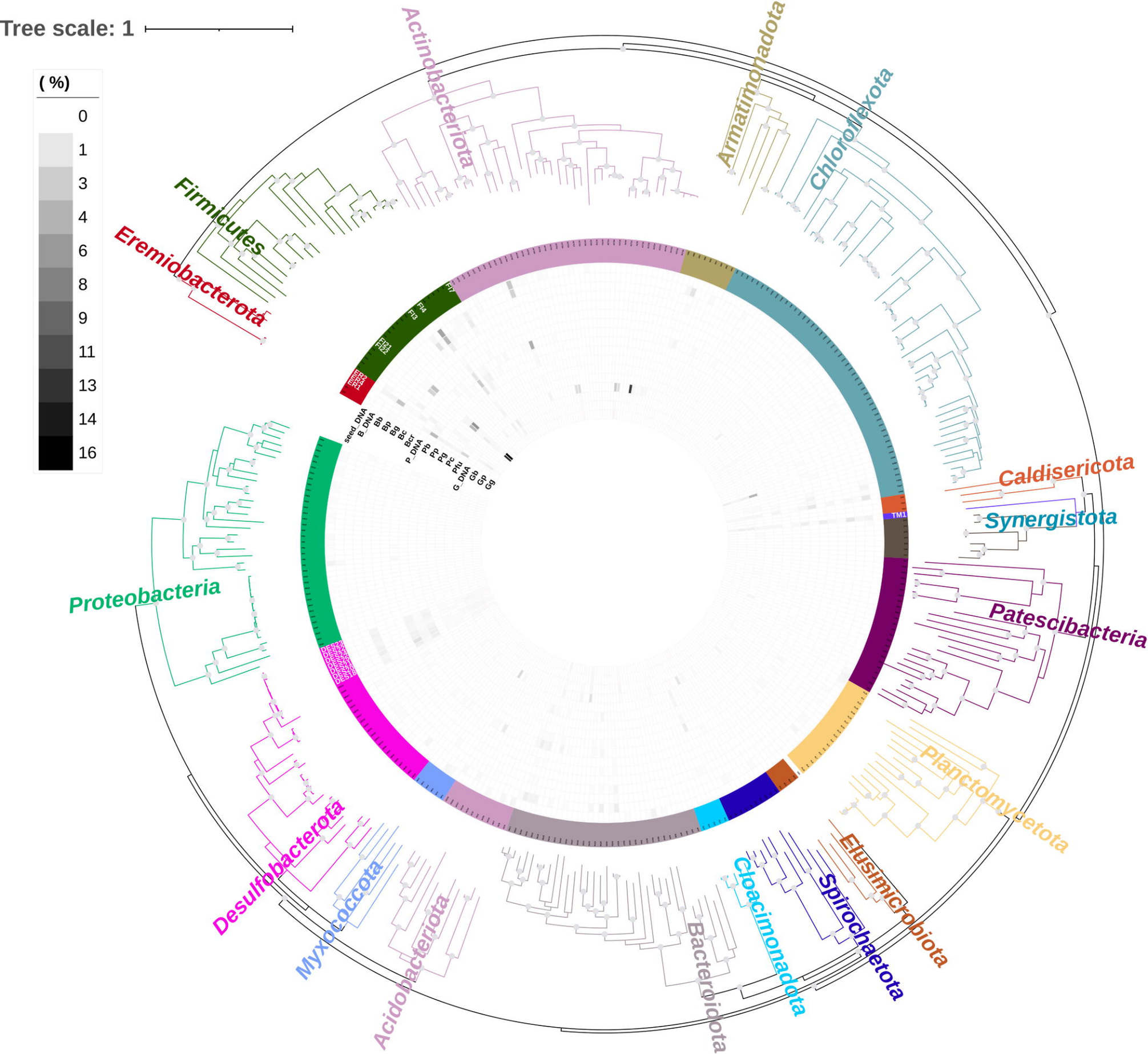

Tree scale: 1
( %)
0
1
3
4
6
8
9
11
13
14
16
Actinobacteriota
Armatimonadota
Chloroflexota
Firmicutes
Eremiobacterota
Caldisericota
Synergistota
Patescibacteria
Proteobacteria
Planctomycetota
Desulfobacterota
Myxococcota
Acidobacteriota
Bacteroidota
Cloacimonadota
Spirochaetota
Elusimicrobiota
seed_DNA
B_DNA
Bb
Bp
Bg
Bc
Bcr
P_DNA
Pb
Pp
Pg
Pc
Pfu
G_DNA
Gb
Gp
Gg
TM1

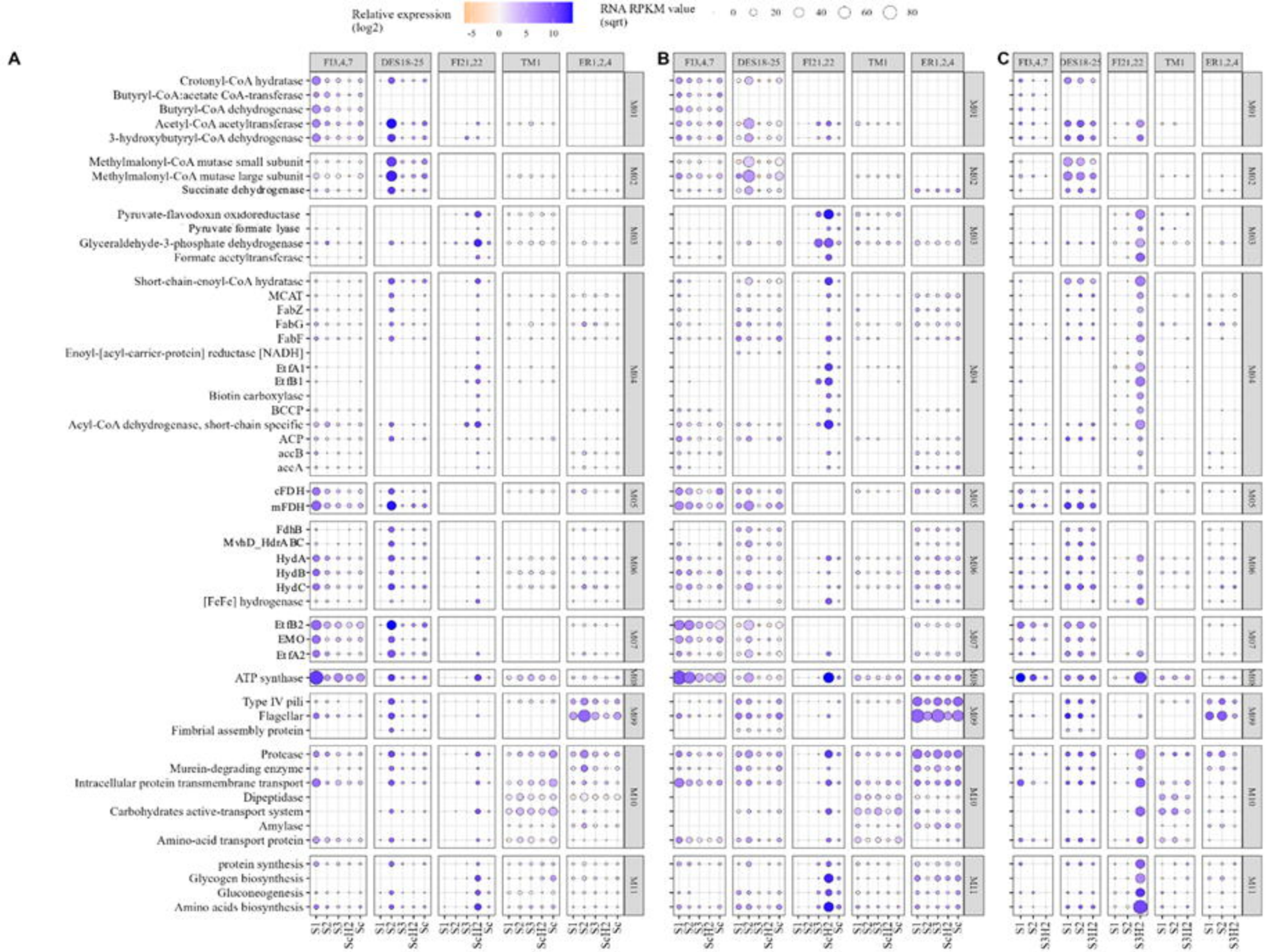

Relative expression (log2)
-5 0 5 10
RNA RPKM value (sqrt)
0 20 40 60 80
A
B
C
FI3,4,7
DES18-25
FI21,22
TM1
ER1,2,4
Crotonyl-CoA hydratase
Butyryl-CoA:acetate CoA-transferase
Butyryl-CoA dehydrogenase
Acetyl-CoA acetyltransferase
3-hydroxybutyryl-CoA dehydrogenase
Methylmalonyl-CoA mutase small subunit
Methylmalonyl-CoA mutase large subunit
Succinate dehydrogenase
Pyruvate-flavodoxin oxidoreductase
Pyruvate formate lyase
Glyceraldehyde-3-phosphate dehydrogenase
Formate acetyltransferase
Short-chain-enoyl-CoA hydratase
MCAT
FabZ
FabG
FabF
Enoyl-[acyl-carrier-protein] reductase [NADH]
EtfA1
EtfB1
Biotin carboxylase
BCCP
Acyl-CoA dehydrogenase, short-chain specific
ACP
accB
accA
cFDH
mFDH
FdhB
MvhD_HdrABC
HydA
HydB
HydC
[FeFe] hydrogenase
EtfB2
EMO
EtfA2
ATP synthase
Type IV pili
Flagellar
Fimbrial assembly protein
Protease
Murein-degrading enzyme
Intracellular protein transmembrane transport
Dipeptidase
Carbohydrates active-transport system
Amylase
Amino-acid transport protein
protein synthesis
Glycogen biosynthesis
Gluconeogenesis
Amino acids biosynthesis
M01
M02
M03
M04
M05
M06
M07
M08
M09
M10
M11
S1 S2 S3 S3H2 Sc

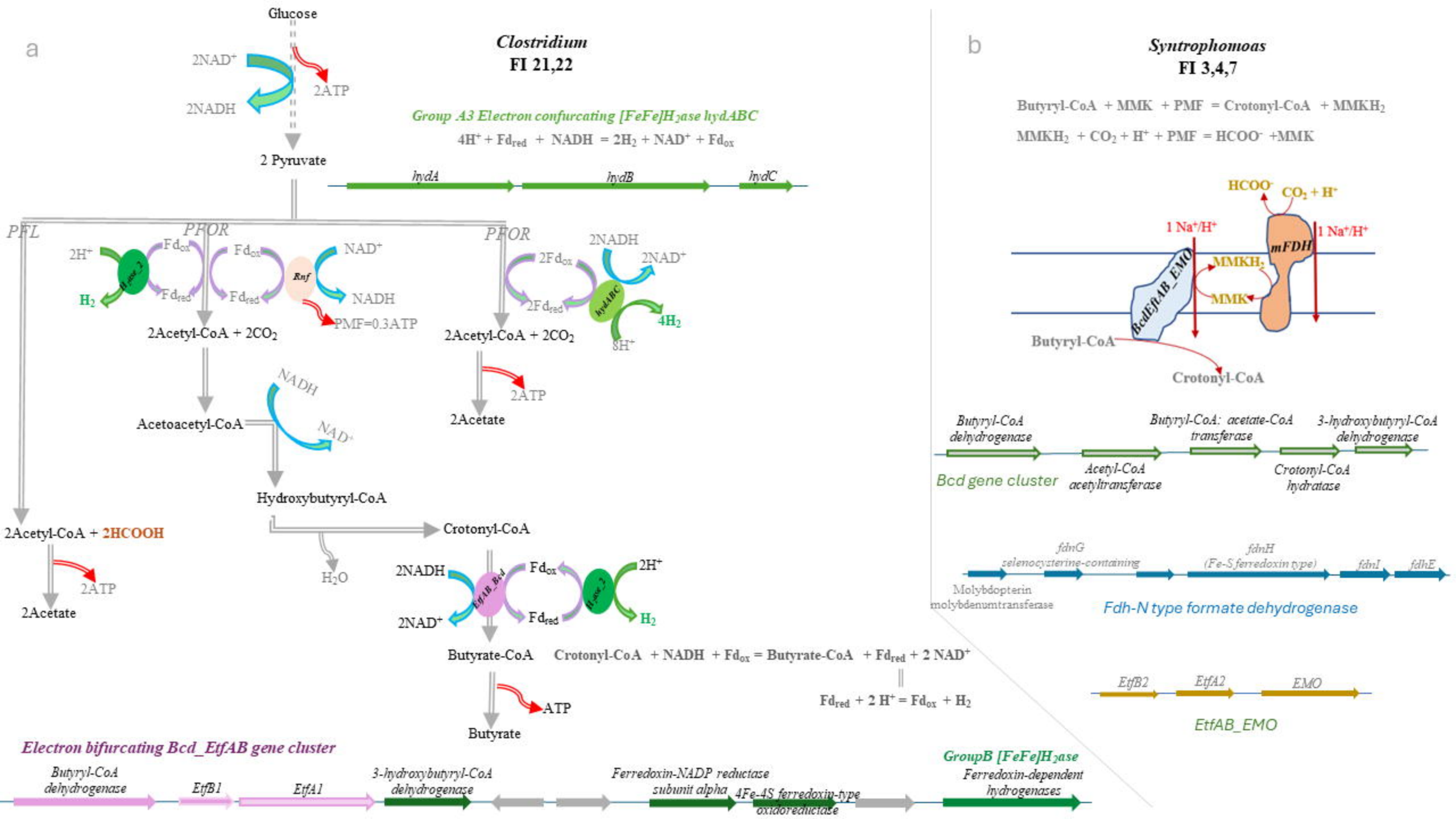
a
Glucose
2NAD+
2NADH
2ATP
2 Pyruvate
Clostridium
FI 21,22
Group A3 Electron confurcating [FeFe]H2ase hydABC
4H+ + Fdred + NADH = 2H2 + NAD+ + Fdox
hydA
hydB
hydC
PFL
PFOR
PFOR
2H+
H2
Fdox
Fdred
Rnf
NAD+
NADH
PMF=0.3ATP
2NADH
2NAD+
2Fdox
2Fdred
hydABC
4H2
8H+
2Acetyl-CoA + 2CO2
2Acetyl-CoA + 2CO2
2ATP
2Acetate
NADH
NAD+
Acetoacetyl-CoA
Hydroxybutyryl-CoA
2Acetyl-CoA + 2HCOOH
2ATP
2Acetate
H2O
Crotonyl-CoA
2NADH
2NAD+
EtfAB_Bcd
Fdox
Fdred
2H+
H2
Butyrate-CoA
Crotonyl-CoA + NADH + Fdox = Butyrate-CoA + Fdred + 2 NAD+
Fdred + 2 H+ = Fdox + H2
ATP
Butyrate
Electron bifurcating Bcd_EtfAB gene cluster
Butyryl-CoA dehydrogenase
EtfB1
EtfA1
3-hydroxybutyryl-CoA dehydrogenase
Ferredoxin-NADP reductase subunit alpha
4Fe-4S ferredoxin-type oxidoreductase
GroupB [FeFe]H2ase
Ferredoxin-dependent hydrogenases
b
Syntrophomoas
FI 3,4,7
Butyryl-CoA + MMK + PMF = Crotonyl-CoA + MMKH2
MMKH2 + CO2 + H+ + PMF = HCOO- +MMK
HCOO-
CO2 + H+
1 Na+/H+
1 Na+/H+
mFDH
BcdEftAB_EMO
MMKH2
MMK
Butyryl-CoA
Crotonyl-CoA
Butyryl-CoA dehydrogenase
Butyryl-CoA: acetate-CoA transferase
3-hydroxybutyryl-CoA dehydrogenase
Bcd gene cluster
Acetyl-CoA acetyltransferase
Crotonyl-CoA hydratase
fdnG selenocysterine-containing
fdnH (Fe-S ferredoxin type)
fdnI
fdhE
Molybdopterin molybdenumtransferase
Fdh-N type formate dehydrogenase
EtfB2
EtfA2
EMO
EtfAB_EMO

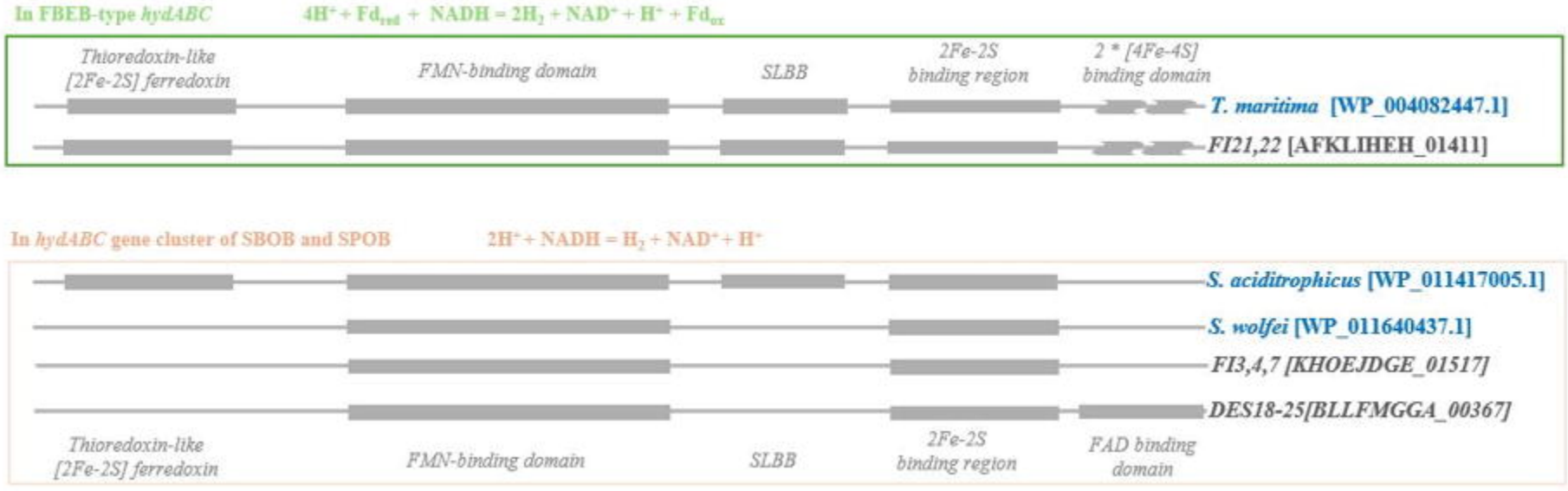
In FBEB-type hydABC
4H⁺ + Fd_red + NADH = 2H₂ + NAD⁺ + H⁺ + Fd_ox
Thioredoxin-like [2Fe-2S] ferredoxin
FMN-binding domain
SLBB
2Fe-2S binding region
2 * [4Fe-4S] binding domain
T. maritima [WP_004082447.1]
FI21,22 [AFKLIHEH_01411]
In hydABC gene cluster of SBOB and SPOB
2H⁺ + NADH = H₂ + NAD⁺ + H⁺
S. aciditrophicus [WP_011417005.1]
S. wolfei [WP_011640437.1]
FI3,4,7 [KHOEJDGE_01517]
DES18-25[BLLFMGGA_00367]
Thioredoxin-like [2Fe-2S] ferredoxin
FMN-binding domain
SLBB
2Fe-2S binding region
FAD binding domain

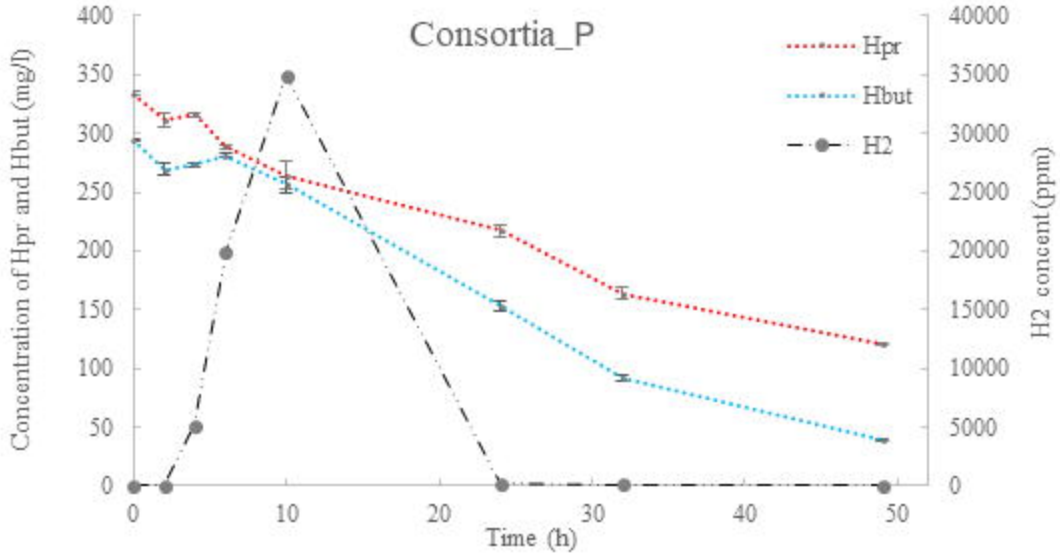


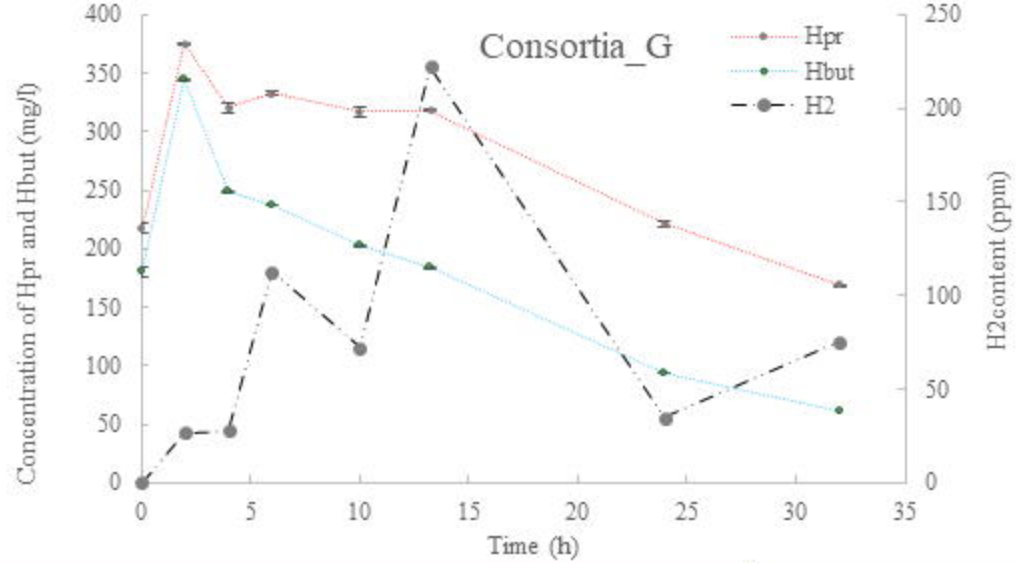


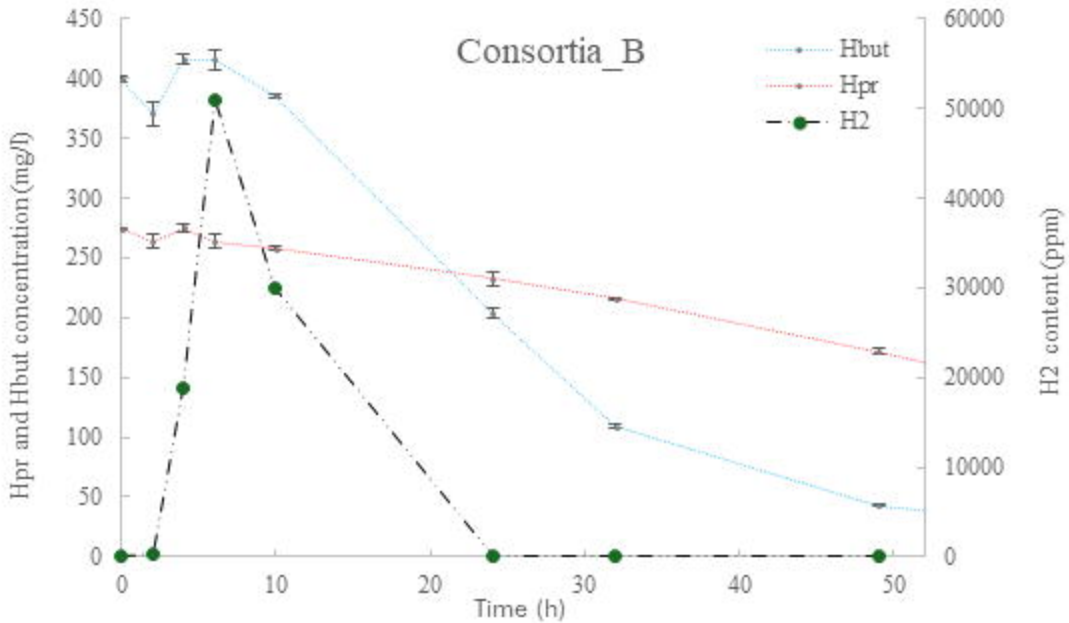


| Consortia-P fed with G:B:P=1:1:1 | | | | | | Gibbs free energy change[1] for the acetogenic degradation of | | |
|---|---|---|---|---|---|---|---|---|
| Time (h) | $H_2$ (ppm) | Hpr (mg/l) | n-Hbut (mg/l) | HAc (mg/l) | iso-Hbut (mg/l) | Hpr | n-Hbut | iso-Hbut |
| 2 | 20 | 312±2 | 269±2 | 17±1 | 9±0.1 | -23 | -38 | -29 |
| 4 | 5114 | 316±2 | 273±2 | 55±0.2 | 18±0.1 | 23 | 50 | 57 |
| 6 | 19903 | 289±12 | 281±7 | 89±2 | 20±5 | 35 | 73 | 80 |
| 10 | 34937 | 264±5 | 257±5 | 133±5 | 24±1 | 40 | 81 | 87 |
| 24 | 174 | 217±5 | 153±2 | 255±8 | 40±1 | 2 | 4 | 7 |
| 32 | 116 | 164±1 | 91±1 | 248±1 | 38±0.2 | -1 | -2 | 1 |
| 49 | 51 | 120±1 | 39±0.3 | 199±2 | 34±0.4 | -7 | -13 | -13 |

| Consortia-B fed with G:B:P=1:1:1 | | | | | | Gibbs free energy change for the acetogenic degradation of | | |
|---|---|---|---|---|---|---|---|---|
| Time (h) | $H_2$ (ppm) | Hpr (mg/l) | n-Hbut (mg/l) | HAc (mg/l) | iso-Hbut (mg/l) | Hpr | n-Hbut | iso-Hbut |
| 2 | 353 | 264±6 | 399±10 | 29±0.6 | 1±0.03 | 7 | 16 | 16 |
| 4 | 18747 | 275±4 | 371±4 | 70±1 | 34±0.1 | 71 | 79 | 79 |
| 6 | 50975 | 264±6 | 416±9 | 95±2 | 43±0.3 | 87 | 96 | 96 |
| 10 | 30000 | 258±1 | 386±4 | 101±1 | 21±0.1 | 42 | 50 | 50 |
| 24 | 103 | 232±5 | 203±1 | 174±5 | 0 | -7 | -3 | -3 |
| 32 | 107 | 216±0.4 | 109±1 | 182±2 | 0 | -5 | -3 | -3 |
| 49 | 51 | 172±2 | 43±4 | 91±1 | 0 | -16 | -16 | -16 |

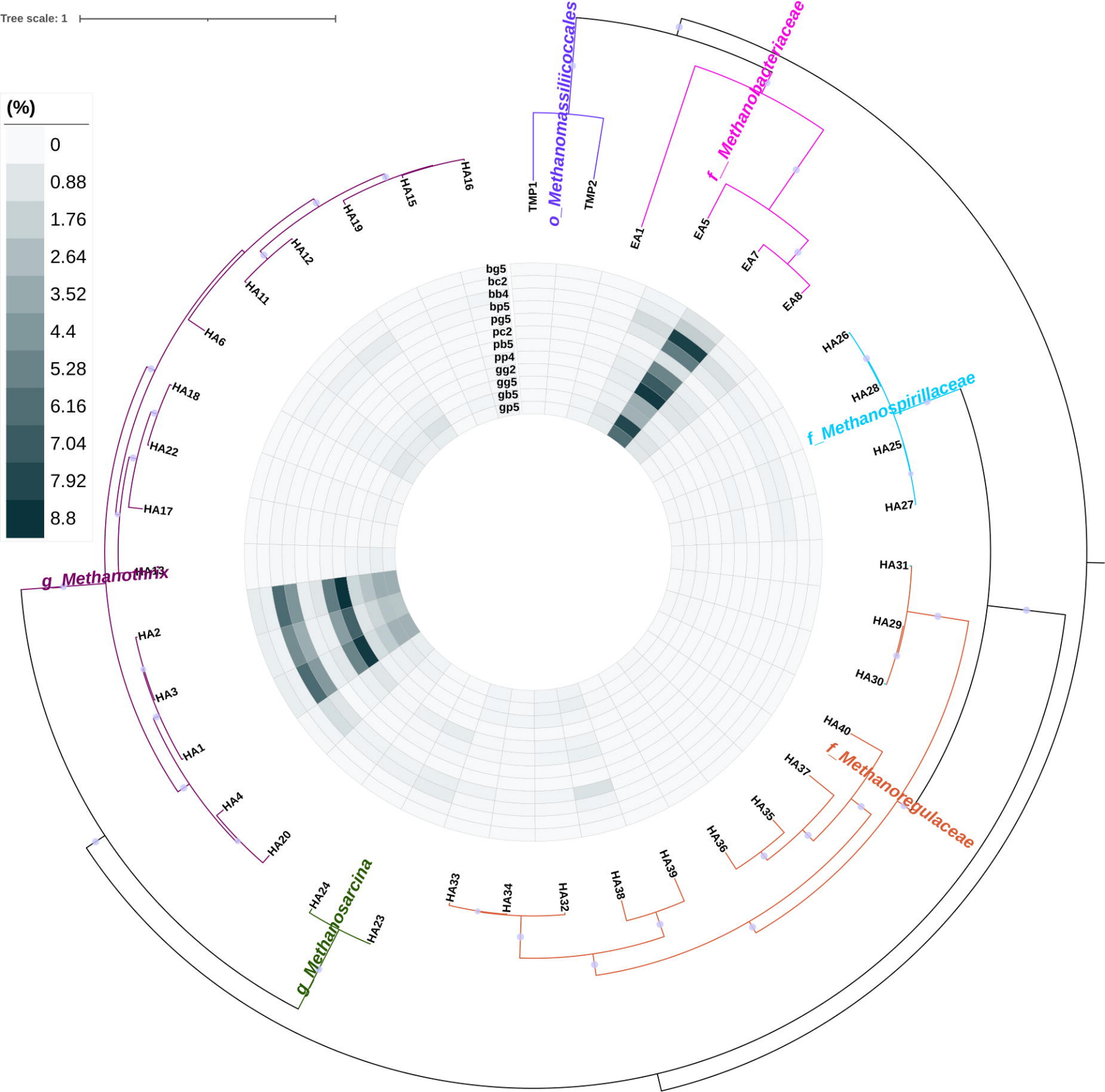
Tree scale: 1
(%)
0
0.88
1.76
2.64
3.52
4.4
5.28
6.16
7.04
7.92
8.8
o_Methanomassiliicoccales
f_Methanobacteriaceae
f_Methanospirillaceae
f_Methanoregulaceae
g_Methanothrix
g_Methanosarcina
TMP1
TMP2
EA1
EA5
EA7
EA8
HA16
HA15
HA19
HA12
HA11
HA6
HA18
HA22
HA17
HA13
HA2
HA3
HA1
HA4
HA20
HA24
HA23
HA33
HA34
HA32
HA38
HA39
HA36
HA35
HA37
HA40
HA30
HA29
HA31
HA27
HA25
HA28
HA26
bg5
bc2
bb4
bp5
pg5
pc2
pb5
pp4
gg2
gg5
gb5
gp5

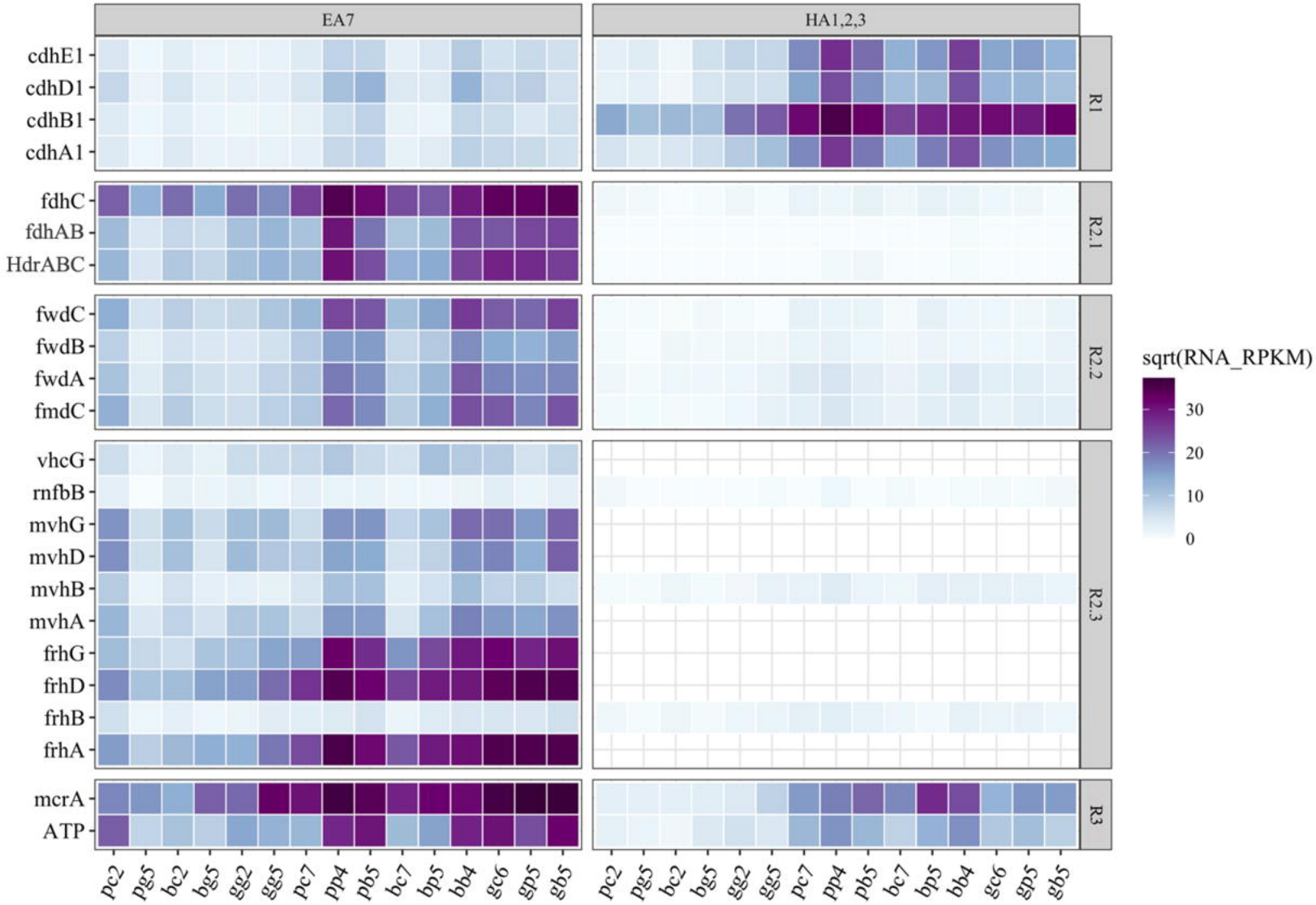
EA7
HA1,2,3
cdhE1
cdhD1
cdhB1
cdhA1
fdhC
fdhAB
HdrABC
fwdC
fwdB
fwdA
fmdC
vhcG
rnfbB
mvhG
mvhD
mvhB
mvhA
frhG
frhD
frhB
frhA
mcrA
ATP
R1
R2.1
R2.2
R2.3
R3
pc2
pg5
bc2
bg5
gg2
gg5
pc7
pp4
pb5
bc7
bp5
bb4
gc6
gp5
gb5
sqrt(RNA_RPKM)
30
20
10
0

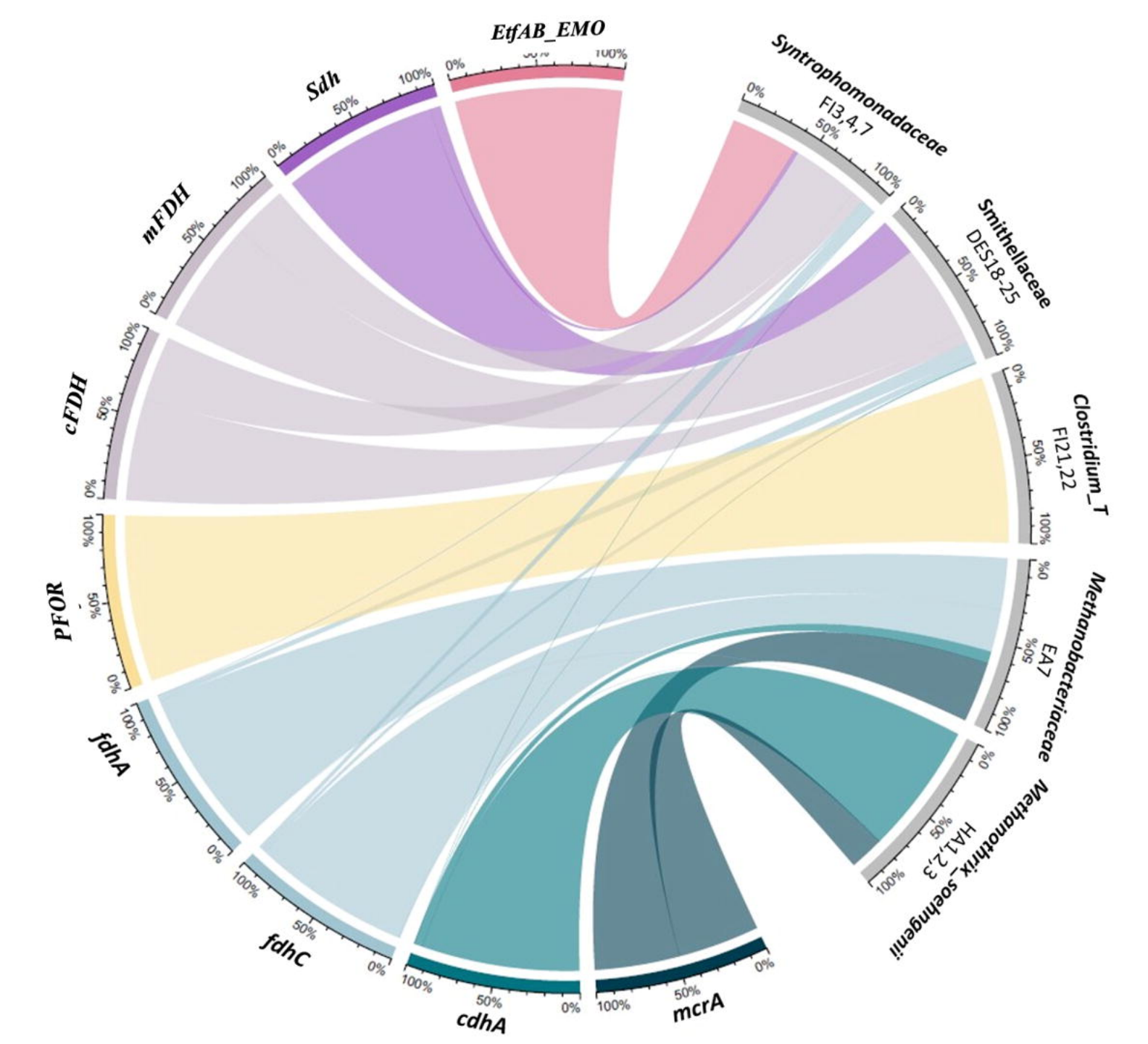
EtfAB_EMO
Syntrophomonadaceae
FI3,4,7
Smithellaceae
DES18-25
Clostridium_T
FI21,22
Methanobacteriaceae
EA7
Methanothrix_soehngenii
HA1,2,3
mcrA
cdhA
fdhC
fdhA
PFOR
cFDH
mFDH
Sdh
0%
50%
100%